Anode supported planar solid oxide fuel cells with the large size of 30 cm × 30 cm via tape-casting and co-sintering technique

Yejian Xue[*], *Wanbing Guan, Changrong He, Wu Liu, Jianxin Wang, Shanshan Sun, Zhenwei Wang, Weiguo Wang*[**]

Division of Fuel Cell and Energy Technology, Ningbo Institute of Material Technology and Engineering, Chinese Academy of Sciences (CAS), Ningbo 315201, PR China

chinaXiv:201705.00415v1

ARTICLE INFO

Keywords:
Anode supported
Large size
Solid oxide fuel cell
Tape casting
Co-sintering technique

ABSTRACT

In this work, the NiO−8YSZ/8YSZ half-cells for planar ASCs with the large size of 30 cm × 30 cm are prepared by optimizing both the sintering characteristics and the sintering temperature. The shrinkage rates, open porosities and flexural strength of the half-cells are investigated systematically. The large size half-cells which are prepared by the tape-casting, co-sintering and two-step sintering method show the optimal comprehensive performances with the sintering temperature being 1350 °C. The NiO+8YSZ/8YSZ/LSM+8YSZ anode-supported single cells are obtained at the sintering temperature of 1050 °C. The maximum measurement power at output voltage of 0.8 V of the two cells and 1.6 V of the stack can reach 32.6 W, 34.7 W and 67.3 W, respectively. The two-cells stack is successively discharged under constant current of 5 A for 316 h with the degradation rate of 1.58% kh^{-1} and 30 A for 1161 h with no degradation at the temperature of 750 °C. The large size ASCs show the good mechanical strength and an acceptable degradation.

Introduction

Solid oxide fuel cells (SOFCs) convert the chemical energy from fuel directly into electrical energy have attracted much attention due to its high electrical efficiency, environmental friendly, and fuel flexibility [1,2]. SOFCs include the type of planar and tubular. Recently, the planar type SOFCs become the development trend for the commercialization application because of its high power density and low production cost [3]. However, the planar SOFCs are divided into the electrolyte-supported and anode-supported type [4]. The anode supported cells (ASCs) has higher powder density due to the thin electrolyte with the thickness of approximately 10 μm [5].

Though the tape casting and the co-sintering technology is a cost-effective technique for fabricating large-scale ceramic substrates and multilayered structures [6–10], it is still difficult to acquire a flat anode-supported half-cell, especially for the large-size ASCs. During the fabricating process, the mismatch between the material properties of the anode-support and the electrolyte causes the warpage of cells [11,12]. The different layers are already in strong tension and

* *Corresponding author*. Tel.: +86 574 8632 4572; fax: +86 574 8668 5702.
** *Corresponding author*. Tel.: +86 574 8791 8363; fax: +86 574 8668 5702.
E-mail addresses: xueyejian@nimte.ac.cn (Y. Xue), wgwang@nimte.ac.cn (W. Wang).

others in compression [13]. These high residual stresses can result in the single cell more fragile during the stacking process. Although there has been reported that a large-scale cell with the area of 22 cm × 33 cm was used to study the internal reforming on ASCs [14]. However, it is still necessary to research on the preparation of large-size flat anode-support fuel cells.

In this work, the tape-casting, co-sintering, two-step sintering, and screen printing technique have been used to fabricate the flat anode-supported planar SOFCs with the large size of 30 cm × 30 cm. Here, the large-size Ni-8YSZ/8YSZ/8YSZ-LSM ASCs with the electrolyte thickness of 10 μm were successfully fabricated. In addition, their sintering properties, microstructures, mechanical strengths, and electrochemical properties were investigated systematically.

Experimental

The material of 8 mol%Y_2O_3-stabilized ZrO_2 (8YSZ) and NiO was purchased from Qingdao Terio Corporation of China and Sinopharm Chemical Reagent Co. Ltd. of China, respectively. The powder of $(La_{0.7}Sr_{0.3})_{0.98}MnO_3$ (LSM) was prepared by the solid–liquid composite method [15]. For the preparation of the anode-support slurry, the mixture of 2-butanone and ethanol with a volume ratio of 2:1, polyvinylbutyral (PVB) and dibutyl-phthalate (DBP) were used as the solvent, the binder and the plasticizer, respectively. Then the mixture of 8YSZ and NiO, solvent, binder and plasticizer with the ratio of 15:20:60:3:2 was ball milled for 24 h to obtain the uniform slurry. For fabrication of the NiO–8YSZ/8YSZ half-cell, the size of 38 cm × 38 cm anode-supports green tape were prepared by the conventional tape-casting method followed by multilayer lamination. The active anode layer with the thickness of 20 μm and the electrolyte with the thickness of 10 μm were prepared successively with the spraying, co-sintering and two-step sintering method. The half-cells were sintered by the two-step sintering process at the temperature of 1100 °C for 2 h and 1350 °C for 4 h, respectively.

To study the pyrolysis behavior and the phase evolution of the anode support green tapes dried at 40 °C, TG-DTA analysis was carried out with heating velocity of 5 °C min^{-1} in air. For studying the sintering behaviors of the anode-support green tape, the 5 cm × 5 cm samples were prepared with the same method, and then sintered at the different temperatures. The shrinkage rates of the half cells were measured by equation (1) with the formula as follows:

$$\text{shrinkage}(\%) = \frac{l_0 - l_1}{l_0} \times 100\% \tag{1}$$

where l_0 and l_1 are the lengths of the tape-cast green tapes and sintered half cells, respectively. For studying the flexural strength, the half cells with the dimensions of 4 mm × 1.4 mm × 36 mm were also prepared with the same method mentioned before. For each sintered temperature, 10 half-cell samples were selected and measured in a screw-driven universal testing machine (Instron4483, Instron, USA) with a span of 20 mm, at the cross-head moving velocity of 0.3 mm min^{-1}. The flexural strength values were obtained from the maximum load, according to the standard recommendations (ASTM-C1161, 1994). The microstructure of the single cell was observed by the scanning electron microscope (SEM, Hitachi T-1000).

The cathode slurry was prepared by mixing the powders of LSM (50 wt.%) and 8YSZ (50 wt.%) in terpineol solvent by ball milling. The cathode slurry was printed on the side of electrolyte by the method of screen printing. After drying at the temperature of 80 °C for 24 h, the single cells with the active areas of 625 cm^2 were sintered at the temperature of 1050 °C for 2 h, and the thickness of the cathode was approximately 20 μm.

Before the two-cell short stack performance tests, the NiO slurry and Ag paste were printed on the anode and cathode surface of the single cells for the current collection, respectively. The stack was reduced at 850 °C for 2 h and tested at temperature of 750 °C using the stainless steel 430 (SS430) as interconnect. Air and dry hydrogen were used as an oxidant and fuel, respectively. The two cells and stack performances were evaluated by the current–voltage (I–V) and current–-power (I–P) curves at the temperature of 750 °C. Lastly, the stack was successively discharged under constant current of 5 A for 316 h and 30 A for 1161 h at 750 °C.

Results and discussion

The TG/DTA curves of the half-cell green tape, the shrinkage rates of the half cells, and the photographs of the sintered half-cells are presented in Fig. 1. As can be seen in Fig. 1a, the loss in weight of approximately 21.4% for the TG curve is due to the thermal decomposition of the binder and plasticizer in the green tape accompanied by the sharp exothermic reaction in DTA curve. The exothermic peaks are approximately 380 and 450 °C. With an increase of temperature, no further changes in weight and heat are detected, indicating that the half-cell is in relatively stable state. The shrinkage rates of the half cells sintered at different temperature are showed in Fig. 1b. The shrinkage rates at the temperature from 100 to 900 °C are very small (less than 2%), and increasing rapidly from 2% to 20.5% from 900 °C to 1350 °C, then increasing slowly to 21.4%. The photos of the samples sintered at different temperatures show in Fig. 1c are also further confirmed the sintering process. It is the carbide and combustion process of the binder and plasticizer before the temperature of 500 °C, and then the sintering process of the NiO–8YSZ composite ceramic material from 900 to 1400 °C. Thus the two temperature range of 300–500 °C and 900–1100 °C are very important to fabricate anode-supported half-cells due to the combustion and sintering process. In addition, thermal behavior of the sample was characterized by a NETZSCH DIL 402C pushrod dilatometer from room temperature to 1450 °C with a heating rate of 3 °C min^{-1}. From the Fig. 1d, the analysis of the shrinkage rate curves of the sample pre-sintered at 1100 °C for 2 h revealed that the densification at the temperature of approximately 1150 °C and the maximum shrinkage rate was achieved at the temperature of 1225 °C.

Samples for the open porosity testing were also prepared with the same method, then sintered in air at different

chinaXiv:201705.00415v1

chinaXiv:201705.00415v1

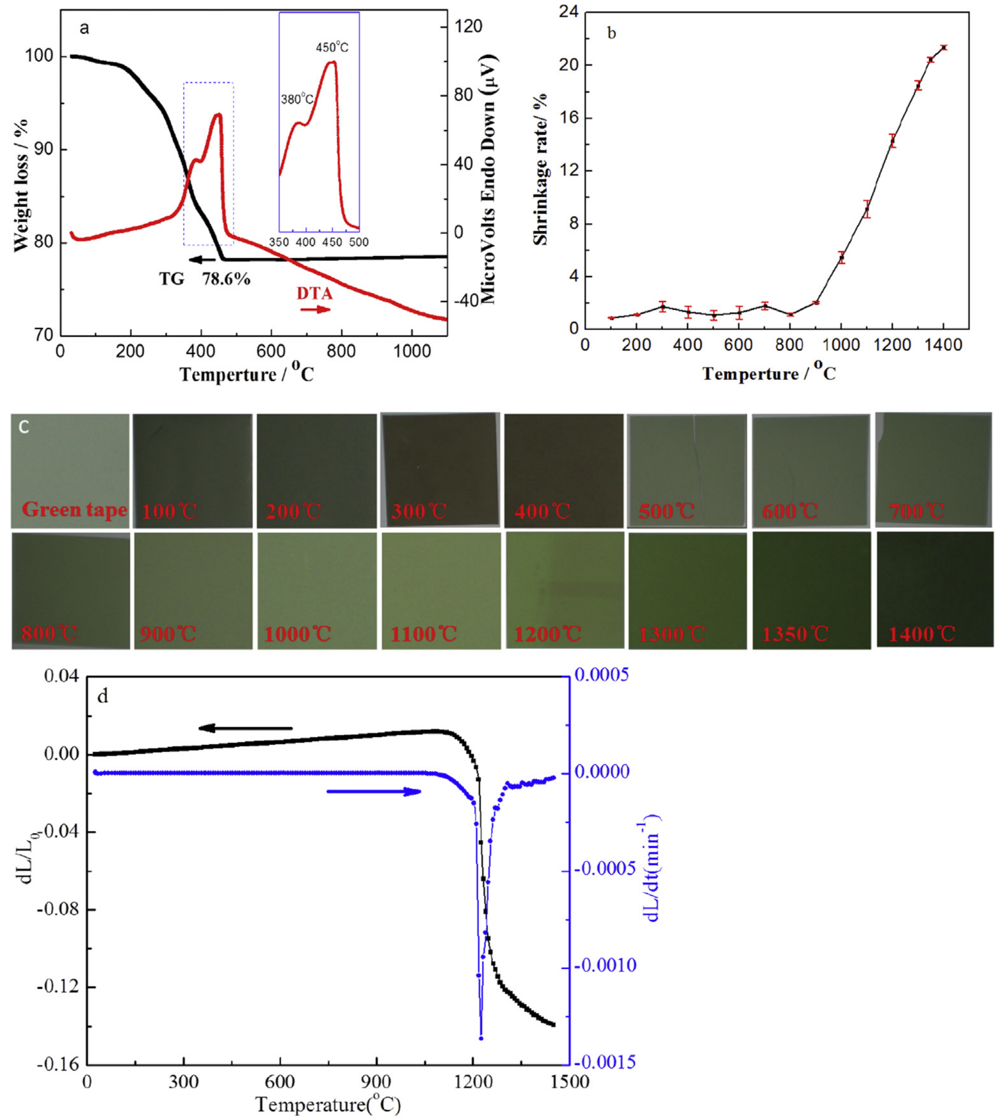

Fig. 1 – The TG/DTA curves of the anode support green tape (a), the shrinkage rate of the half cells (b), the photographs of the sintered anode support (c) at the different sintering temperatures, and the shrinkage rate curves of the sample (d).

temperature for 4 h and half of the specimens were reduced in H_2 at 850 °C for 2 h. The open porosities of unreduced and reduced samples test with the Archimedes method are shown in Fig. 2. It is shown that the porosity of the unreduced and reduced samples decreasing from 20% and 36.8% to 8.6% and 24.3%, under the sintering temperature from 1200 °C to 1400 °C, respectively. From the Fig. 2, the porosity of unreduced and reduced half-cell is both decreased rapidly after the sintering temperature of 1300 °C. The flexural strength of the half-cells as a function of the sintering temperature is also shown in Fig. 2. It can be seen that the flexural strength of the half-cell increases from 186 MPa to 283 MPa under the sintering temperature from 1200 °C to 1400 °C. The flexural strength of the samples sintered at 1350 °C and 1400 °C are 265 MPa and 283 MPa, which is much higher that of the samples sintered at the same temperature in the references [24–26]. Therefore, the co-sintering temperature of 1350 °C is

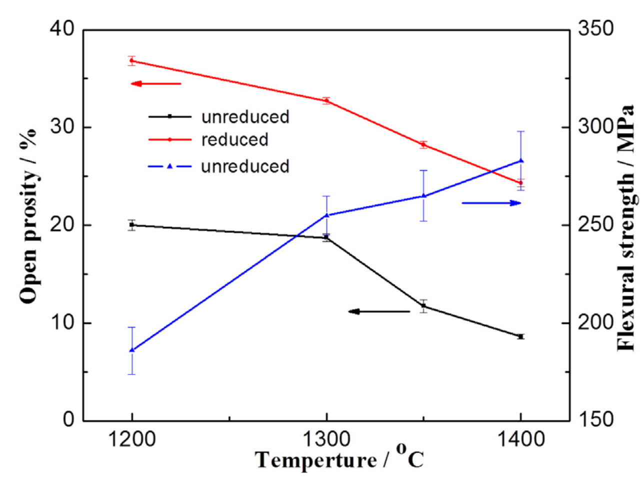

Fig. 2 – The open porosities and flexural strength of the half-cells sintered at the different temperatures.

more suitable for the fabrication of NiO–8YSZ/8YSZ anode support half-cells.

The sintering process of the half-cell, the photo and SEM micrographs of the anode-support single cell sintered at 1350 °C, and the photo graph of the two-cell stack are shown in the Fig. 3. The two-step sintering method was used to fabricate the anode-support half-cells, and the sintering curves were shown in Fig. 3a. During the first sintering stage, the temperature rate is 33 °C h^{-1} from 300 °C to 1100 °C with the purpose of the completely combustion of organic additive and partial sintering of ceramic particles, and then keeps the temperature of 1100 °C for 2 h. During the second sintering stage, the sintered cover plate was used. And the temperature rate is 100 °C h^{-1} from room-temperature to 1100 °C, then with the rate of 30 °C h^{-1} from 1100 °C to 1350 °C and keeps the temperature of 1350 °C for 4 h. The flat NiO–8YSZ/8YSZ half-cells for planar ASCs with the large size of 30 cm × 30 cm were successfully by the process of tape-casting, co-sintering, and two-step sintering. While the half-cell fabricated by the one-step sintering process was bending seriously. It is difficult to evaluate the flatness of the cell with irregular warpage showed in Fig. 3b. Fig. 3c and d shows the SEM micrographs of the large-size half-cell co-sintered at 1350 °C. The thickness of the 8YSZ electrolyte and active anode layer are around 10 μm and 20 μm, respectively, and the 8YSZ electrolyte is dense. The area of NiO–8YSZ/8YSZ/LSM-8YSZ full cell is 30 × 30 cm^2, and the active area of the cathode is 25 × 25 cm^2 (show in Fig. 3e). Fig. 3f shows the photograph of the two-cell short stack with the large size ASCs using the stainless steel 430 (SS430) as interconnect.

Fig. 4 shows the I–V, I–P, and aging curves of the two-cell stack tested at the temperature of 750 °C with the active electrode area of 625 cm^2 and H_2 flow of 5000 sccm. In this work, the SS430 testing device was used to test the electrochemical properties of the cells and stack. It is well known that the resistance of stainless steel leads of the testing device

chinaXiv:201705.00415v1

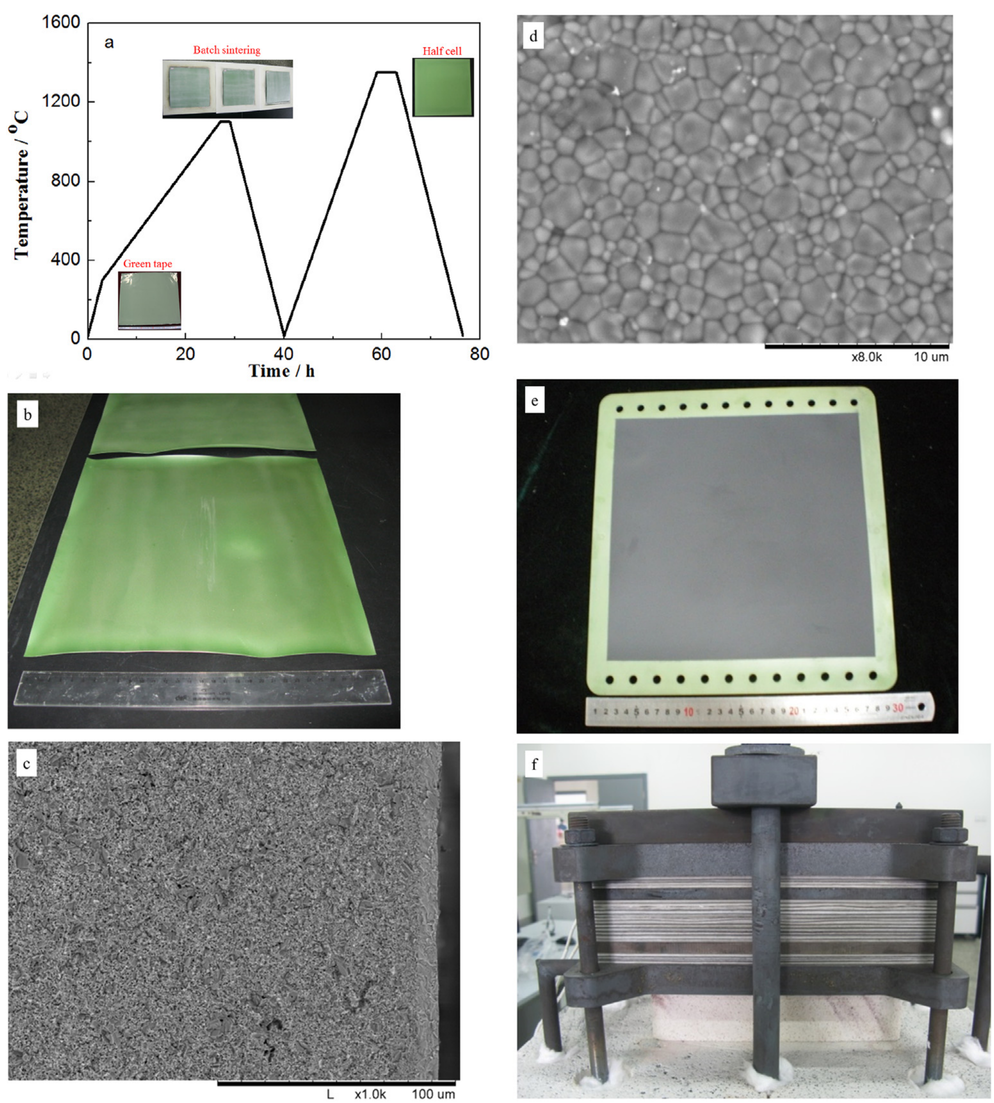

Fig. 3 – The sintering process of the half-cell (a); photograph of the half-cell sintered by one-step sintering process (b); SEM micrographs of the half-cell sintered at 1350 °C: cross-section (c) and electrolyte surface (d); photo graph of the full-cell sintered at 1050 °C (e), photo graph of the two-cell stack (f).

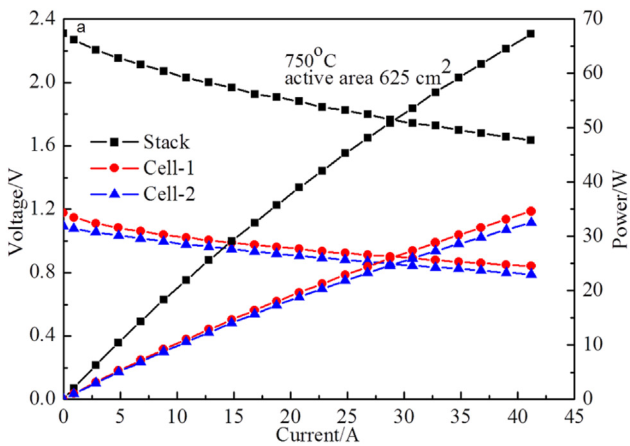

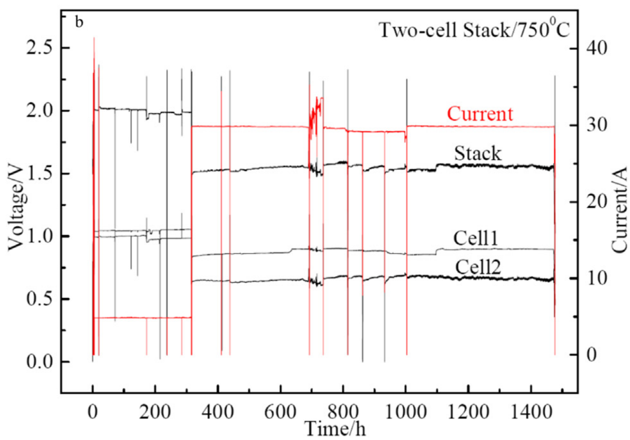

Fig. 4 – Current–voltage (I–V) and current–power (I–P) curves of the large size ASCs tested at the 750 °C(a), and the degradation curve of the ASCs operated at constant current for 1477 h at 750 °C(b).

is much higher than that of Pt or Ag plate/mesh, especially at the high temperature. So the output voltage of cells and stack is occupied by the steel leads of the external circuit, and the maximum power cannot be obtained when the testing current becomes larger. From the Fig. 4a, It can be seen that the open current voltage (OCV) of the two cells and short stack reach 1.123 V, 1.186 V and 2.309 V, respectively. It means that the 8YSZ electrolyte layer was dense without significant gas cross over, and the performance of the sealing components was excellent [16,17]. It also shows that the maximum measurement power (P_{max}) of the two cells and short stack reach 32.6 W, 34.7 W and 67.3 W at the discharge current of 41.2 A, respectively. Fig. 4b shows the aging curves of the two-cell stack with the large size ASCs for 316 h at a constant current of 5 A and 1161 h at a constant current of 30 A, respectively. In order to fully activate the cells, a low current of 5 A was used to age for 316 h. The output voltage of the cells and short stack slightly decreases from 0.989 V to 0.985 V, 1.011 V to 1.005 V, and 2.000 V to 1.990 V after 316 h, corresponding to the degradation rate of 1.28% kh^{-1}, 1.88% kh^{-1}, and 1.58% kh^{-1}, respectively. The Cr element diffused into the electrode under the high temperature, which maybe the degradation mechanism of the cells and stack during the long-term discharging [18,19]. In addition, the high temperature corrosion of stainless steel test-house is likely to be another reason for cell performance degradation, which can lead to significantly increases in resistance of the cell [20,21]. Then the stack was aged at a constant current of 30 A for 1161 h. From the Fig. 4b, it can be seen that there is no degradation on the cells and the short stack during the second constant current discharging. This may be because of the better contact between interconnect and cells during the aging process, or the entirely reduction of the NiO in anode [22,23] due to the very large size which lead the H_2 flow difficult to uniformly distribute in the cells. This indicates that planar ASCs with a large area of 30 cm × 30 cm can operate at 750 °C with a low degradation rate.

Conclusions

In this study, the flat NiO–8YSZ/8YSZ half-cells for planar ASCs with the large size of 30 cm × 30 cm were obtained by optimizing both the sintering characteristics and the sintering temperature of green-tapes. By optimizing the sintering process, the large size half-cells were prepared with the tape-casting, co-sintering, and two-step sintering method at 1350 °C for 4 h. The thickness of the 8YSZ electrolyte and the active anode layer are about 10 μm and 20 μm, respectively, and the 8YSZ electrolyte is dense. Then, the flexural strength and porosity of the half-cells were investigated in detail. After that, the NiO+8YSZ/8YSZ/LSM+8YSZ anode-supported single cells were prepared at the sintering temperature of 1050 °C. And the maximum measurement power at output voltage of 0.8 V of the two cells and 1.6 V of the stack could reach 32.6 W, 34.7 W and 67.3 W, respectively. Lastly, the two-cells stack was successively discharged under constant current of 5 A for 316 h with the degradation rate of 1.58% kh^{-1} and 30 A for 1161 h with no degradation at the temperature of 750 °C. The results indicated that the large size NiO–8YSZ/8YSZ/8YSZ-LSM anode supported single cells showed the good mechanical strength and low degradation rate. To the best of our knowledge, so large anode supported single cells are firstly reported, and this work is expected to open a new pathway to prepare the large size anode supported single cells for the commercial application.

Acknowledgement

The authors are grateful for the financial supports from the Ningbo Natural Science Foundation (No. 2014A610033, No. 2015A610251).

REFERENCES

[1] Minh NQ. Ceramic fuel cells. J Am Ceram Soc 1993;76(3):563–88.
[2] Mark Ormerod R. Solid oxide fuel cells. Chem Soc Rev 2003;32:17–28.

chinaXiv:201705.00415v1

chinaXiv:201705.00415v1

[3] Singhal SC, Kendall L. High temperature solid oxide fuel cells: fundamentals, design and applications. NY: Elsevier; 2003pp.197–228.

[4] Xue YJ, Miao H, He CR, Wang JX, Liu M, Sun SS, et al. Electrolyte supported solid oxide fuel cells with the super large size and thin ytterbia stabilized zirconia substrate. J Power Sources 2015;279:610–9.

[5] Timurkutluk B, Mat MD. Effects of anode fabrication parameters on the performance and redox behavior of solid oxide fuel cells. J Power Sources 2014;258:108–16.

[6] Shen ZM, Zhu XD, Le SR, Sun W, Sun KN. Co-sintering anode and Y_2O_3 stabilized ZrO_2 thin electrolyte film for solid oxide fuel cell fabricated by co-tape casting. Int J Hydrogen Energy 2012;37:10337–45.

[7] Le SR, Sun KN, Zhang NQ, Zhu XD, Sun HX, Yuan YX, et al. Fabrication and evaluation of anode and thin Y_2O_3-stabilized ZrO_2 film by co-tape casting and co-firing technique. J Power Sources 2010;195:2644–8.

[8] Jin C, Mao YC, Zhang NQ, Sun KN. Fabrication and characterization of Ni-SSZ gradient anodes SSZ electrolyte for anode-supported SOFCs by tape casting and co-sintering technique. Int J Hydrogen Energy 2015;40:8433–41.

[9] Mucke R, Menzler NH, Buchkremer HP, Stover D. Cofiring of thin zirconia films during SOFC manufacturing. J Am Ceram Soc 2009;92(S1):S95–102.

[10] Charlas B, Frandsen HL, Brodersen K, Henriksen PV, Chen M. Residual stresses and strength of multilayer tape cast solid oxide fuel and electrolysis half-cells. J Power Sources 2015;288:243–52.

[11] Azari K, Vaghasloo YA, Mohandesi JA, Ghobadzadeh AH. The effect of cell shape on the warpage in solid oxide fuel cells. J Power Sources 2015;279:64–71.

[12] Molla TT, Ni DW, Bulatova R, Bjork R, Bahl C, Pryds N, et al. The effect of cell shape on the warpage in solid oxide fuel cells. J Am Ceram Soc 2014;97(9):2965–72.

[13] He CR, Wang WG, Wang JX, Xue YJ. Effect of alumina on the curvature, youngs modulus, thermal expansion coefficient and residual stress of planar solid oxide fuel cells. J Power Sources 2011;196:7639–44.

[14] H. T. Lim, C. Yang, S. C. Hwang, Y. J. Choi, Experimental study of internal reforming on large-area anode supported solid oxide fuel cells, Fuel Cells, doi: 10.1002/fuce.201400070.

[15] Liu M, He CR, Wang WG, Wang JX. Synthesis and characterization of 10Sc1CeSZ powders prepared by a solid-liquid method for electrolyte-supported solid oxide fuel cells. Ceram Int 2014;40:5441–6.

[16] Luo J, Yan D, Fang DW, Liang FL, Pu J, Chi B, et al. Electrochemical performance and thermal cyclic ability of industrial-sized anode supported planar solid oxide fuel cells. J Power Sources 2013;224:37–41.

[17] Chen G, Guan GQ, Abliz S, Kasai Y, Abudula A. Rapid degradation mechanism of Ni-CGO anode in low concentrations of H_2 at a high current density. Int J Hydrogen Energy 2011;36:8461–7.

[18] Leonard MLE, Amendola R, Gannon PE, Shong WJ, Liu CK. High-temperature (800 °C) dual atmosphere corrosion of electroless nickel-plated ferritic stainless steel. Int J Hydrogen Energy 2014;39:15746–53.

[19] Hosseini N, Abbasi MH, Karimzadeh F, Choi GM. Development of $Cu_{1.3}Mn_{1.7}O_4$ spinel coating on ferritic stainless steel for solid oxide fuel cell interconnects. J Power Sources 2015;273:1073–83.

[20] Grolig JG, Froitzheim J, Svensson JE. Coated stainless steel 441 as interconnect material for solid oxide fuel cells: evolution of electrical properties. J Power Sources 2015;284:321–7.

[21] Grolig JG, Froitzheim J, Svensson JE. Coated stainless steel 441 as interconnect material for solid oxide fuel cells: oxidation performance and chromium evaporation. J Power Sources 2014;248:1007–13.

[22] Hatae T, Matsuzaki Y, Yamashita S, Yamazaki Y. Destruction modes of anode-supported SOFC caused by degrees of electrochemical oxidation in redox cycle. J Electrochem Soc 2010;157(5):B650–4.

[23] Hatae T, Matsuzaki Y, Yamashita S, Yamazaki Y. Current density dependence of changes in the microstructure of SOFC anodes during electrochemical oxidation. Solid State Ionics 2009;180:1305–10.

[24] Sato K, Naito M, Abe H. Electrochemical and mechanical properties of solid oxide fuel cell i/YSZ anode fabricated from NiO/YSZ composite powder. J Ceram Soc Jpn 2011;119(1395):876–83.

[25] He CR, Wang WG. Alumina doped Ni/YSZ anode materials for solid oxide fuel cells. Fuel Cells 2009;9(5):630–5.

[26] Horri BA, Selomulya C, Wang H. Characteristics of Ni/YSZ ceramic anode prepared using carbon microspheres as a pore former. Int J Hydrogen Energy 2012;37:15311–9.